Accurate electron channeling contrast analysis of dislocations in fine grained bulk materials

H. Mansour,[a] J. Guyon,[a,b] M.A. Crimp,[c] N. Gey,[a,b] B. Beausir[a,b] and N. Maloufi[a,b,d,*]

[a]*Laboratoire d'Étude des Microstructures et de Mécanique des Matériaux (LEM3), UMR CNRS 7239,
Université de Lorraine, 57045 Metz, France*
[b]*Laboratory of Excellence on Design of Alloy Metals for low-mAss Structures (DAMAS), Université de Lorraine, France*
[c]*Department of Chemical Engineering & Materials Science, 2527 Engineering Building, Michigan State University, East Lansing,
MI 48824, United States*
[d]*Département de Physique et d'Électronique, Université de Lorraine, 57070 Metz, France*

Non-destructive, comprehensive dislocations characterization in fine grained Interstitial-Free Steel was realized for the first time by Accurate Electron Channeling Contrast Imaging "A-ECCI" in a Scanning Electron Microscope. Conventional Transmission Electron Microscopy $\mathbf{g} \cdot \mathbf{b} = 0$ invisibility criterion and trace analysis were applied to determine Burgers vectors and line directions in this bulk material. This approach relies on the live collection of High Resolution Selected Area Channeling Patterns "HR-SAC-Ps" using an innovative procedure to rock the beam with a remarkable spatial resolution of about 1 μm.
© 2014 Acta Materialia Inc. Published by Elsevier Ltd. All rights reserved.

Electron channeling contrast imaging (ECCI) has seen increasing use for imaging dislocation structures in the near-surface region of bulk materials, thin films, and many substrates [1–11]. This is in part due to the now widespread availability of high quality field emission gun scanning electron microscopes (FEG-SEMs). Nevertheless, the characterization of crystallographic aspects of these dislocation structures using ECCI remains difficult, despite contrast analysis using the well known transmission electron microscopy $\mathbf{g} \cdot \mathbf{b} = 0$ and $\mathbf{g} \cdot \mathbf{b} \mathbf{x} \mathbf{u} = 0$ invisibility criteria having been demonstrated many years ago [12–16]. The difficulty in applying these criteria lies in accurately orienting specimens to well defined "2-beam" channeling conditions. For large single crystal specimens, electron channeling patterns (ECPs) can be used to establish the channeling conditions by orienting the optic axis of near the edge of a distinct channeling band [17–18]. For polycrystalline materials, such an approach requires that the channeling pattern be collected from an area that lies within the grain of interest. This has historically been achieved by collecting a selected area channeling patter (SACP) [19]. Unfortunately most of the recently developed FEG-SEMs no longer offer the ability to collect SACPs. In the rare microscope configuration where it is still available, the pattern collection area of about five microns in diameter makes quantitative analysis of dislocations using ECCI difficult. Indeed, the SACP should ideally be collected from as small an area as possible, as any significant rotations across the grain, most commonly from geometrically necessary dislocations, will distort the pattern, making it difficult to identify the optimum channeling bands [20].

Electron backscattered diffraction (EBSD) offers an alternative approach for collecting diffraction information with much higher spatial resolutions than SACP. However, applying EBSD to setting up specific channeling conditions is not straightforward. This is because EBSD provides orientations on high tilted crystals (typically 70°) with absolute orientations accurate to

* Corresponding author at: Laboratoire d'Étude des Microstructures et de Mécanique des Matériaux (LEM3), UMR CNRS 7239, Université de Lorraine, 57045 Metz, France.; e-mail: nabila.maloufi@univ-lorraine.fr

approximately 1–2° [21]. In contrast, ECCI requires the crystal orientation to be controlled relative to the electron beam trajectory (optic axis) in the range of 0.1° [19]. Furthermore, while ECCI can be carried with the specimen tilted to the EBSD orientation, the resulting images contain significant topographical contrast, suffer from image foreshortening, and can suffer from varying focal depths. Carrying out ECCI with the sample in the low tilt position (for a review of these two ECCI configurations see [22]) using a pole piece mounted or retractable backscattered electron detector over comes these problems and is more conducive to *in-situ* studies. Gutierrez-Urruti et al. have made use of EBSD orientation analysis to predict the specimen stage tilts and rotations necessary to bring a crystal in to optimum channeling conditions for ECCI at low tilts, a procedure known at controlled electron channeling contrast imaging, cECCI [23]. Because of the uncertainty introduced by the accuracy limitations of EBSD and due to the uncertainly of the SEM stage control, it is not clear if the objective channeling conditions are achieved; it is necessary to adjust the orientation to achieve optimum contrast, and the exact deviation from the Bragg condition, **s**, cannot be assessed.

In this paper, we propose a novel approach to control the channeling conditions for performing ECCI. It is based on a new method for collecting high angular and spatial resolution SACPs. We demonstrate that these HR-SACPs, combined with simulated EBSD patterns, can be used for TEM style contrast analysis of dislocations from even relatively fine grained polycrystals. This is evidenced on an interstial free (IF) steel by orienting the sample to a series of known channeling conditions, and subsequently analyzing the dislocation contrast. Finally, we highlight the need for these HR-SACPs, in combination with simulated EBSD patterns, for accurately setting up the channeling conditions.

This new approach to optimizing channeling conditions, referred to here as Accurate ECCI (A-ECCI), is based on the live acquisition of HR-SACPs collected with an innovative procedure to rock the beam that we have developed for the GEMINI-type FEG electron column. To carry out this rocking, the beam is first deviated from the center of a selected aperture, which results in the electron beam being shifted far from the area of interest, but striking the sample at an angle. Secondly, the electron beam is shifted back to the area of interest using the beam shift control. This process is repeated sequentially, resulting in the beam being rocked on the area of interest, with the HR-SACP being collected as a function of rocking angle. The detailed beam rocking procedure is described in a coming paper, which also includes some typical application examples that demonstrate attractive features of this rocking approach [24]. Especially noteworthy is the resulting spatial resolution of about 1 μm for an angular range of more than 4° [24].

Figures 1 and 2 present for the first time typical HR-SACPs collected with the Zeiss AURIGA 40 FIB SEM on a (0001) GaN single crystal and on a polycrystalline 2%Si-IF Steel respectively. The HR-SACPs were collected using a large four-quadrant Si-diode backscattered electron detector. The microscope was operated at 20 kV using a 10 mm working distance and an electron beam spot of ≈2 nm. Similar conditions were applied
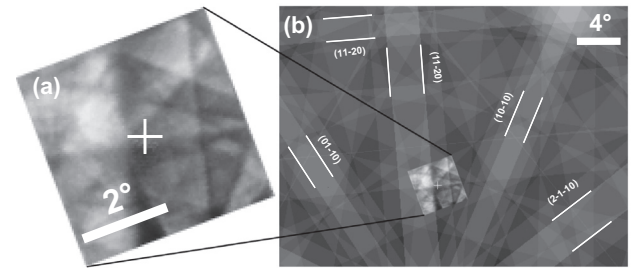
Figure 1. (a) Typical HR-SACP collected from (0001) GaN showing an angular range of ∼4°. The cross indicates the microscope optic axis. (b) The GaN HR-SACP superimposed on an EBSD pattern simulated for 0° tilt. The HR-SACP contains enough information to index the diffraction planes based on the simulated diffraction pattern.
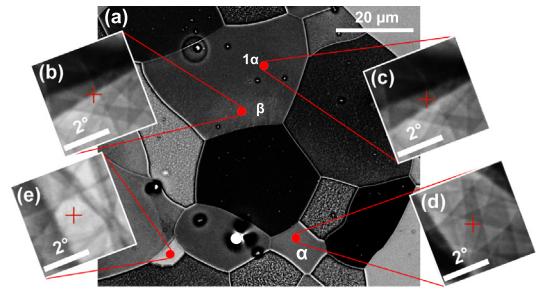
Figure 2. (a) BSE micrograph from the 2%Si IF-steel. The HR-SACPs (b, c, d, e) were collected from large (1α, 1β) and small grains (grain 3(e) about 4 μm in width and grain 2(d) about 10 μm in width). The contrast in grain 1 is due to the disorientation between area 1α and area 1β. The disorientation between the two areas 1α and 1β measured by HR-SACPs (c) and (b) is estimated at 0.3°.

for ECCI. Prior to the HR-SACP collection, the samples were tilted to 70° to determine the orientations of the regions of interest by EBSD (Quantax CrystAlign Bruker system). These orientations were used to simulate the EBSD patterns (the equivalent of SACPs) corresponding to the 0° tilt, using the Bruker system.

Figure 1a shows an HR-SACP collected from the GaN single crystal. On its own, the angular range of approximately 4° is not adequate to identify the various channeling bands in the SACP. However, when overlaid on the simulated pattern shown in Figure 1b, the HR-SACP can be readily aligned with simulated bands, allowing accurate indexing of the channeling bands in the HR-SACP. Furthermore, the high angular resolution of the HR-SACP allows the sample to be tilted and/or rotated to align the optic axis (center of the HR-SACP pattern) with high accuracy, in the range of 0.1° (this is consistent with the angular accuracy typically given for SACPs [19]). For the purposes of carrying out ECCI, this means that two-beam channeling conditions can be set up with high accuracy, and with the fine spatial resolution of the HR-SACPs [24], ECCI can be carried out with excellent control, even in fine polycrystals.
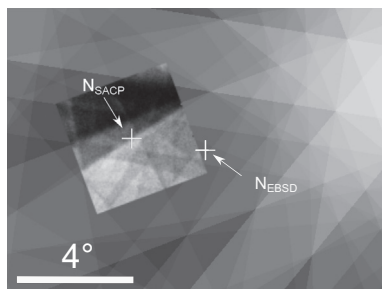
The procedure outlined above for the GaN single crystal was then applied to a polycristalline 2%Si IF-steel slightly deformed in tension. The specimen surface was first mechanically polished and then finished electrolytically. This second example, illustrated in Figure 2, demonstrates a number of features of the HR-SACP approach.

First, the HR-SACPs shown in Figure 2b and c were collected from the same grain, but at locations approximately 10 μm from each other. The subtle shifts in the channeling patterns relative to the optic axis (red +) reveal a disorientation of 0.3°. This highlights the sharpness of the HR-SACPs so that small orientation variations can be detected. The relative angular precision here is significantly better than that from EBSD technique [24].

The second feature evident in Figure 2 is that the HR-SACPs can be collected from very small grains. In particular, Figure 2e shows a pattern collected from a grain approximately 4 μm in the narrow dimension. Note that the all of the patterns show sharp, straight channeling bands with no evidence of any information coming from outside the grain of interest. These HR-SACPs were acquired without any difficulty on the smallest grains observed in the microstructure (Fig. 2a). Our experience shows that the HR-SACPs collected at about 1 μm from the grain boundaries are easily indexed in conjunction with the pattern simulations. This is in agreement with the 1 μm spatial resolution of the HR-SACP technique demonstrated in [24].

The need for the HR-SACPs, in addition to the EBSD, for accurately setting up the channeling conditions is illustrated in Figure 3. This figure compares the specimen normal (N_{EBSD}) determined experimentally using EBSD with the sample tilted to the 70° to the specimen normal determined using HR-SACP (N_{SACP}) after the sample was tilted to 0° (N_{SACP} is the optic axis at the 0° position, precluding errors in specimen mounting, common to both positions). It is clear that there is a discrepancy in these two orientations of about 2°. This error is a direct consequence of the accuracy of the EBSD technique, known to be in the range of 1–2°, and inaccuracies in the stage tilt to 70° [21]. To set up electron channeling conditions accurately for a given family of crystal planes, and in particular to satisfy the dislocations invisibility criteria used to determine the Burger's vectors, one must rotate and tilt the sample. The error shown here suggests that, solely based on EBSD orientation information, it will be difficult to accurately control the channeling conditions through tilt and/or rotations from the EBSD position without additional information such as that provided by the HR-SACPs.

We used this optimized procedure on the 2%Si IF-steel for the demonstration of the comprehensive characterization of dislocations through contrast analysis. At low deformation, the dislocations in the bcc IF-Steel are expected to be primarily $\mathbf{b} = 1/2 \langle 111 \rangle$ screw dislocations. The conventional TEM $\mathbf{g} \cdot \mathbf{b} = 0$ invisibility criterion was applied to analyze these dislocations (where $\mathbf{b}$ is the Burgers vector and $\mathbf{g}$ the diffraction vector).

Grain 1 in Figure 2 had an orientation near the [1 1 1] zone axis, as shown in the simulated EBSD pattern of the surface normal in Figure 4a. In this orientation, the three other $\langle 111 \rangle$ dislocation line directions are inclined roughly 20 degrees from parallel with the sample surface with projections approximately 120 degrees from one another (Fig. 4b). These line directions, shown as fading dotted lines indicating their sense of inclination, are labeled on the stereographic projection. Figure 4a also shows four HR-SACPs superimposed on the simulated EBSD pattern that were used to set up channeling conditions for the four ECC images shown in Figures 4c–f. The sample was tilted up to 15° and rotated to reach these four different $\mathbf{g}$ vectors. Two sets of dislocations, with line directions labeled $\mathbf{a}$ and $\mathbf{b}$ and consistent with two of the nearly in-plane $\langle 111 \rangle$ line directions, are visible in the ECC images. Because ECCI dislocation contrast is strong near the surface and decreases as the dislocations project further below the surface, it is
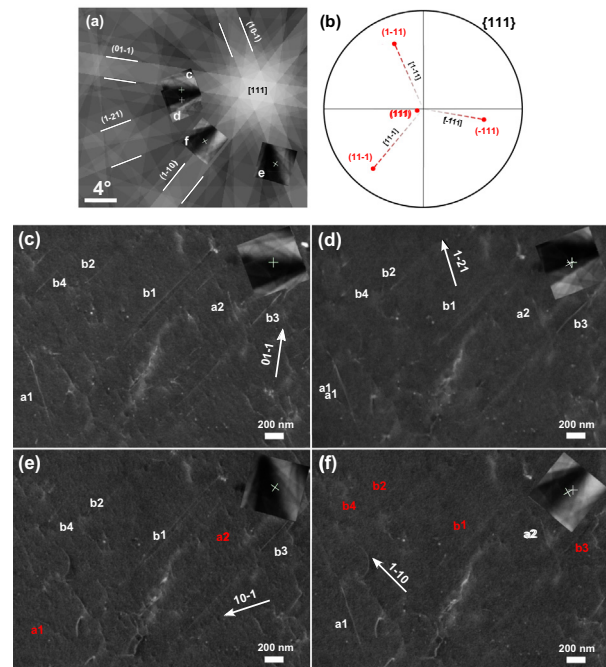
Figure 4. Characterization of dislocations in grain 1 (Fig. 2a) of the 2%Si IF-steel. (a) Four HR-SACPs superimposed on a simulated EBSD pattern. (b) Stereographic projection showing the {1 1 1} poles. The fading dotted lines represent the directions of the inclined $\langle 111 \rangle$ screw dislocations and show how the channeling contrast from screw dislocations with these three $\langle 111 \rangle$ line directions will decrease as the dislocations extend below the sample surface. (c–f) ECCI images of dislocations collected using the four channeling conditions shown in (a): (c) $\mathbf{g} = 01\text{-}1$; (d) $\mathbf{g} = 1\text{-}21$; (e) $\mathbf{g} = 10\text{-}1$; (f) $\mathbf{g} = 1\text{-}10$. Two dislocation line directions corresponding to $\mathbf{u} = \mathbf{b} = [1\text{-}11]$ (dislocations a) and $[11\text{-}1]$ (dislocations b) are seen. The dislocations are labeled in red where they disappear. (For interpretation of the references to colour in this figure legend, the reader is referred to the web version of this article.)

Figure 3. Comparison of the specimen normal measured by EBSD (shown on the corresponding EBSD pattern simulation) taken with the sample tilted to 70° and the specimen normal (optic axis) measured by HR-SACP at a sample tilt of 0°.

possible to get a sense of the inclination of the dislocations. Thus, dislocations **a** project in to the sample from the upper left to lower right, consistent with the inclination of the [1 -1 1] line direction. Similar analysis of the dislocations **b** shows inclination consistent with the [1 1 -1] line direction (from lower left to upper right). The imaging under the four different channeling conditions reveals contrast variations consistent with the dislocations being ⟨1 1 1⟩ screw dislocations. The dislocations labeled **a1** and **a2**, with line directions [1 -1 1], are visible with $\mathbf{g} = (0\,1\,\text{-}1)$, $\mathbf{g} = (1\,\text{-}1\,0)$, and $\mathbf{g} = (1\,\text{-}2\,1)$ (all for which $\mathbf{g}\cdot\mathbf{b} \neq 0$) and invisible (in red in the Fig. 4e) at $\mathbf{g} = (1\,0\,\text{-}1)$ with $\mathbf{g}\cdot\mathbf{b} = 0$. Likewise, the dislocations labeled **b1–b4**, with line directions of [1 1 -1], are visible with $\mathbf{g} = (0\,1\,\text{-}1)$, $\mathbf{g} = (1\,0\,\text{-}1)$ and $\mathbf{g} = (1\,\text{-}2\,1)$, but invisible (in red in the Fig. 4f) with $\mathbf{g} = (1\,\text{-}1\,0)$. This analysis illustrates that by accurately setting up channeling conditions using HR-SACPs, robust contrast analysis can be carried out in fine polycrystalline materials.

In conclusion, dislocations in fine-grained 2%Si IF-Steel were characterized in terms of Burgers vectors and line directions using a new HR-SACPs assisted A-ECCI procedure. With the remarkable 1 μm spatial resolution of the HR-SACP technique, A- ECCI offers the ability to carry out TEM style contrast analysis for dislocation characterization in fine grained bulk materials. Using this HR-SACP technique in combination with simulated EBSD patterns, direct and precise channeling conditions for ECCI at both low and high tilts are established through specimen stage tilts and rotations. This approach opens the way for robust non destructive characterization of defects in bulk materials and opens a new path to optimizing channeling conditions in a variety of different instruments.

[1] A. Weidner, F. Pyczak, H. Biermann, Mater. Sci. Eng. A 571 (2013) 49–56.

[2] A. Barnoush, Acta Mater. 60 (2012) 1268–1277.
[3] M.A. Crimp, Microsc. Res. Tech. 69 (2006) 374–381.
[4] S. Primig, H. Leitner, W. Knabl, A. Lorich, H. Clemens, R. Stickler, Mater. Sci. Eng. A 535 (2012) 316–324.
[5] J. Ahmed, S.G. Roberts, A.J. Wilkinson, Philos. Mag. 86 (29–31) (2006) 4965–4981.
[6] J. Dluhos, L. Sedlacek, J. Man, in: 21st Int. Conf. Metall. Mater. 2012, pp. 216–220.
[7] Y.N. Picard, R. Kamaladasa, M. De Graef, N.T. Nuhfer, W.J. Mershon, T. Owens, L. Sedlacek, F. Lopour, Microsc. Today 20 (2012) 12–16.
[8] R.J. Kamaladasa, F. Liu, L.M. Porter, R.F. Davis, D.D. Koleske, G. Mulholland, K.A. Jones, Y.N. Picard, J. Microsc. 244 (2011) 311–319.
[9] J.K. Hite, M.A. Mastro, C.R. Eddy Jr., J. Cryst. Growth 312 (2010) 3143–3146.
[10] G. Naresh-Kumar, B. Hourahine, P.R. Edwards, A.P. Day, A. Winkelmann, A.J. Wilkinson, P.J. Parbrook, G. England, C. Trager-Cowan, Phys. Rev. Lett. 108 (2012) 135503.
[11] N. Ferralis, J. Kawasaki, R. Maboudian, C. Carraro, Appl. Phys. Lett. 93 (2008) 191916.
[12] C.J. Humphreys, J.P. Spencer, R.J. Woolf, D.C. Joy, J.M. Titchmarsh, G.R. Booker, in: Proceedings of the 5th Annual SEM Symposium, 1972, pp. 205–214.
[13] M. Pitaval, P. Morin, J. Baudry, E. Vicario, G. Fontaine, Scan Electron. Mic. 1 (1977) 439–444.
[14] P. Morin, M. Pitaval, D. Besnard, G. Fontaine, Philos. Mag. A 40 (1979) 511–524.
[15] J.T. Czernuszka, N.J. Long, E.D. Boyes, P.B. Hirsch, Philos. Mag. Lett. 62 (1990) 227–232.
[16] M.A. Crimp, B.A. Simkin, B.C. Ng, Philos. Mag. Lett. 81 (2001) 833–837.
[17] G.R. Booker, A.M.B. Shaw, M.J. Whelan, P.B. Hirsch, Philos. Mag. 16 (1967) 1185–1191.
[18] J.D. Ayers, D.C. Joy, Acta Metall. 20 (1972) 1371–1379.
[19] D.C. Joy, D.E. Newbury, D.L. Davidson, J. Appl. Phys. 53 (8) (1982) R81–R122.
[20] M. Kaczorowski, W.W. Gerberich, J. Mater. Sci. 26 (1991) 1910–1918.
[21] F.J. Humphreys, J. Mater. Sci. 36 (2001) 3833–3854.
[22] B.A. Simkin, M.A. Crimp, Ultramicroscopy 77 (1999) 65–75.
[23] I. Gutierrez-Urrutia, S. Zaefferer, D. Raabe, Scripta Mater. 61 (2009) 737–740.
[24] J. Guyon, H. Mansour, M.A. Crimp, S. Chalal, N. Gey, N. Maloufi, submitted for publication.